Unique Determination of the Form-Factor Ratio in Radiative Pion Decay

L. E. Piilonen, R. D. Bolton, M. D. Cooper, J. S. Frank, A. L. Hallin,[a] P. Heusi,[b] G. E. Hogan, C. M. Hoffman, F. G. Mariam, R. E. Mischke, V. D. Sandberg, R. A. Williams, and S. L. Wilson
Los Alamos National Laboratory, Los Alamos, New Mexico 87545

V. L. Highland and J. McDonough
Temple University, Philadelphia, Pennsylvania 19122

D. Grosnick and S. C. Wright
University of Chicago, Chicago, Illinois 60637

and

M. Ritter[c]
Hansen Laboratories and Department of Physics, Stanford University, Stanford, California 94305
(Received 9 June 1986)

A new experiment studying radiative pion decay, $\pi^+ \rightarrow e^+ \nu_e \gamma$, has been performed with the Crystal Box detector at the Clinton P. Anderson Meson Physics Facility (LAMPF). From a maximum-likelihood analysis of the Dalitz-plot distribution of 2364 coincident and random events, we obtain a unique value for γ, the ratio of the axial-vector to vector weak pion form factors, of 0.25 ± 0.12. The new world average is $\gamma = 0.39 \pm 0.06$.

PACS numbers: 13.20.Cz, 13.40.Hq

The radiative decay of the charged pion, $\pi^+ \rightarrow e^+ \nu_e \gamma$, is sensitive to strong-interaction corrections when the photon is emitted directly from the weak vertex.[1] The emission can be associated with either the weak vector or axial-vector current; this is usually characterized by the ratio of the associated form factors: $\gamma \equiv F_A/F_V$. Previous experimental efforts to determine γ have yielded ambiguous results and a variety of theoretical calculations have produced a wide spectrum of predictions. In this Letter we present a unique experimental determination of γ. The resolution of the experimental question is timely as progress in understanding the low-energy properties of QCD makes plausible a more reliable calculation in the foreseeable future.

In addition to direct photon emission (structure dependence), the amplitude for this decay contains contributions from QED corrections to the $\pi \rightarrow e\nu$ decay (bremsstrahlung). The decay rate is given by

$$\frac{d^2\Gamma}{dx\,dy} = \frac{d^2\Gamma_B}{dx\,dy} + \frac{d^2\Gamma_{SD}}{dx\,dy} + \frac{d^2\Gamma_I}{dx\,dy},$$

where, in the pion rest frame, $x = 2E_\gamma/m_\pi$ and $y = 2E_e/m_\pi$ and Γ_B, Γ_{SD}, and Γ_I are the contributions from bremsstrahlung, structure dependence, and their interference, respectively. The structure-dependent term is given by

$$\frac{d^2\Gamma_{SD}}{dx\,dy} = \frac{\alpha}{8\pi}\Gamma_{\pi e\nu}\left(\frac{F_V}{f_\pi}\right)^2\left(\frac{m_\pi}{m_e}\right)^2[(1+\gamma)^2(1-x)(x+y-1)^2+(1-\gamma)^2(1-x)(1-y)^2],$$

where f_π is the pion decay constant and $\Gamma_{\pi e\nu}$ is the decay rate[2] for $\pi \rightarrow e\nu$. The vector form factor, calculated[3] from the measured π^0 lifetime[4] by use of the conserved-vector-current hypothesis,[5] is $F_V = 0.0259 \pm 0.0004$.

There have been three previous measurements of γ.[6-8] Each of these experiments measured the decay rate for photons and positrons emerging from π^+ decays at rest with opening angles $\theta_{e\gamma}$ near 180°; this geometry was chosen to suppress contributions from bremsstrahlung. In this region of phase space, the term in the decay rate proportional to $(1+\gamma)^2$ dominates so that the determination of γ has a quadratic ambiguity. A weighted average of the results of Refs. 7 and 8 yields

$$\gamma = 0.41 \pm 0.06, \text{ or } \gamma = -2.36 \pm 0.06.$$

From data with $\theta_{e\gamma}$ away from 180°, one experiment[7] favors the negative solution while the other[8] favors the positive solution. To resolve the ambiguity and allow meaningful comparisons with theoretical predictions, substantially more data with $\theta_{e\gamma}$ away from 180° are needed than were obtained in past experiments.

Our experiment used the Crystal Box detector,[9] which accepted events with $90 < \theta_{e\gamma} < 180°$. The

detector was located in the Clinton P. Anderson Meson Physics Facility (LAMPF) stopped muon channel, which was tuned to transport positive pions of 140 MeV/c. The beam rate was $\sim 6\times10^4$ s^{-1} (average) with a duty factor of $\sim 5.5\%$. Each pion passed through an 11.3-g/cm^2 polyethylene degrader and one of four adjacent 1.6-g/cm^2 scintillation beam counters before reaching the 0.35-g/cm^2 polyethylene stopping target. The Crystal Box detector consisted of 396 NaI(Tl) crystals, 36 plastic scintillation hodoscope counters, and a cylindrical drift chamber surrounding the stopping target. The hardware trigger required a "positron quadrant" [a quadrant of the detector with signals from at least one hodoscope counter and at least one NaI(Tl) crystal's discriminator] and an opposite "photon quadrant" [a quadrant with at least 20 MeV deposited in the NaI(Tl) but no hodoscope-counter signal present] within 50 ns of a signal from one of the beam counters. The data written on magnetic tape for each event included timing and pulse-height information from every scintillation counter and from each NaI(Tl) crystal having at least 0.1 MeV deposited energy, timing information from each drift-chamber cell whose discriminator fired, and information from a system that detected any piled-up energy in each NaI(Tl) crystal.

A total of $\sim 4\times10^{10}$ pions were stopped in the target during the live time of the experiment, yielding 6.91×10^6 triggers. The off-line analysis, which required a track in the drift chamber that intersected the target, more than 48 MeV for either the photon or the positron, and no appreciable piled-up energy in the NaI(Tl), reduced the number of candidate events to 55 840. Further cuts retained only those events with E_e and E_γ in the shaded and cross-hatched regions of the Dalitz plot shown in Fig. 1 (27% pass), with $\theta_{e\gamma}$ between 105° and 180° (94%), with the photon converting in the central columns of the NaI(Tl) crystals (56%), with the total energy $E_{\rm tot}=E_e+E_\gamma+|\mathbf{p}_e+\mathbf{p}_\gamma|$ between 115 and 145 MeV (57%), and with the relative time between positron and photon satisfying $|\Delta t_{e\gamma}|<2$ ns (53%). The remaining 2364 events can be due either to $\pi^+\to e^+\nu_e\gamma$ or to chance coincidences between a photon and a positron.

Coincident events with both high-energy photons and positrons are almost entirely due to $\pi\to e\nu\gamma$. Figure 2 shows the distribution of $\Delta t_{e\gamma}$ for events in the cross-hatched region of the Dalitz plot shown in Fig. 1. The dashed curve in Fig. 2 shows the normalized shape of $\Delta t_{e\gamma}$ for random events, as determined from events in the entire shaded and cross-hatched regions of the Dalitz plot shown in Fig. 1. The width of the coincidence peak, 1.25 ns (FWHM), is consistent with the measured time resolution of the detector.

We can determine γ from the $\pi\to e\nu\gamma$ branching ratio, obtained by dividing the 71 ± 11 coincident events by the product of the number of pions stopped in the target and the $\pi\to e\nu\gamma$ detection efficiency, $N_\pi\epsilon_{e\nu\gamma}$. The efficiency $\epsilon_{e\nu\gamma}$ is a product of the fraction of phase space covered in the cross-hatched region, the geometrical solid angle of the detector (determined from the Monte Carlo simulation described later), and measured rate-dependent detector efficiencies for electrons and photons. The number of pions N_π is proportional to a monitor S_π provided by four of the hodoscope scintillators. The proportionality constant is determined from calibration runs in which events

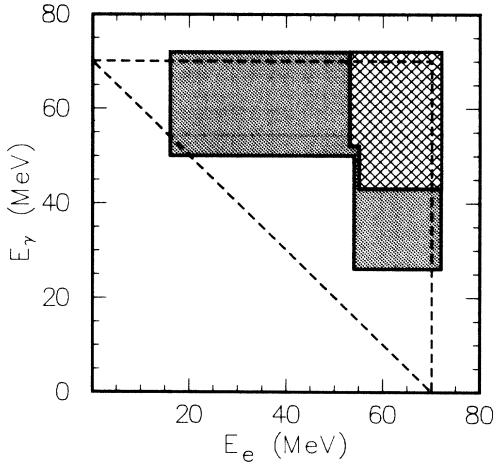

FIG. 1. The regions of the Dalitz plot used in this experiment. The cross-hatched region is used to determine γ from the observed number of $\pi^+\to e^+\nu_e\gamma$ events. The shaded and cross-hatched regions are used in the maximum-likelihood fit. The triangle indicates the limits of phase space assuming perfect measurement resolution.

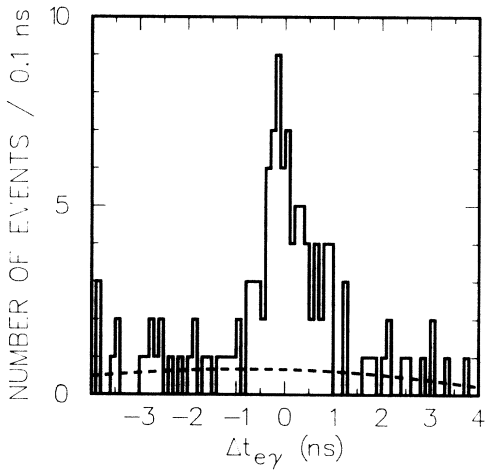

FIG. 2. The measured photon-positron relative time for events in the cross-hatched region of the Dalitz plot shown in Fig. 1. The dashed curve shows the distribution for random events.

were triggered on a single positron. Twenty such runs were taken with a low-energy threshold so that most of the recorded events were from $\mu \rightarrow e\nu\bar{\nu}$. The number of stopping pions for these runs, n_π, was calculated from the 59 ± 10 $\pi \rightarrow e\nu$ (π_{e2}) events in these runs, the π_{e2} branching ratio, and the π_{e2} detection efficiency. Combining this with the pion monitor for these runs, s_π, gives $N_\pi = (s_\pi/n_\pi)S_\pi$ for the $\pi \rightarrow e\nu\gamma$ runs. This method was checked for an independent set of single-positron runs where the π_{e2} content was enriched by imposing in the trigger a threshold on the energy deposited in each row of the NaI(Tl) array, thus selecting positrons above ~ 55 MeV. Here we observe 2970 ± 70 π_{e2} events. As a result of uncertainties in the energy threshold, the π_{e2} detection efficiency in these runs is uncertain to 10%. The results of these two determinations of N_π agree to within 15%. Figure 3 shows the branching ratio for $\pi \rightarrow e\nu\gamma$ in the cross-hatched region of the Dalitz plot in Fig. 1 as a function of γ. The measured value of the branching ratio for this region of the Dalitz plot is indicated by the horizontal line. The value of γ is determined to be either $\gamma = 0.22 \pm 0.15$ or $\gamma = -2.13 \pm 0.15$. This result is consistent with the previous experiments.

The ambiguity in the value of γ is resolved by means of a maximum-likelihood-method fit to the data within the shaded and cross-hatched regions of the Dalitz plot shown in Fig. 1. The likelihood function is defined as

$$L(n_S, \gamma) = \prod_{i=1}^{N} \left[\frac{n_S}{N} S(\mathbf{x}_i, \gamma) + \frac{n_R}{N} R(\mathbf{x}_i) \right],$$

where N is the total number of events, n_S is the estimate of the number of $\pi \rightarrow e\nu\gamma$ events, and $n_R = N - n_S$ is the estimate of the number of random events. The vector $\mathbf{x}$ has components $\Delta t_{e\gamma}$, E_γ, E_e, and $\theta_{e\gamma}$. S and R are the normalized probability distributions for $\pi \rightarrow e\nu\gamma$ and random events, respectively. R is determined from out-of-time events while S comes from $\pi \rightarrow e\nu\gamma$ events generated with a Monte Carlo simulation program.

The Monte Carlo program accurately reproduces the acceptance of the apparatus and the response of the detector to positrons and photons. Electromagnetic showers are simulated with the shower code EGS3.[10] The output of the Monte Carlo program is processed by the same analysis programs as the data.

The best estimate of n_S maximizes the likelihood function for a particular value of γ. In this method, the sensitivity to γ comes entirely from the distribution of $\pi \rightarrow e\nu\gamma$ events over the Dalitz plot; no information on the number of pions decaying in the experiment is used. The maximum value of the likelihood function as a function of γ is shown in Fig. 4. The positive solution for γ is preferred by 2175:1 (i.e., by more than 3.5 standard deviations). The position of the peak of the likelihood function is consistent with the positive value of γ determined above. The value of n_S at the peak of the likelihood function is 179 ± 18 events. This number agrees with the number of $\pi \rightarrow e\nu\gamma$ events obtained by fitting of the $\Delta t_{e\gamma}$ spectrum for all events, $N_{e\nu\gamma} = 218 \pm 67$.

Combining the result from the likelihood fit with the independent result obtained from Fig. 3 above, we obtain the unique solution $\gamma = 0.25 \pm 0.12$. The new world average value is $\gamma = 0.39 \pm 0.06$. This result is in agreement with a recent calculation by Holstein,[11] based on a chiral-symmetric Lagrangean, that predicts $\gamma = 0.46$. Other recent treatments include a quark-model calculation[12] that yields $\gamma \simeq -1.41$ and a calculation based on QCD sum rules[13] that gives

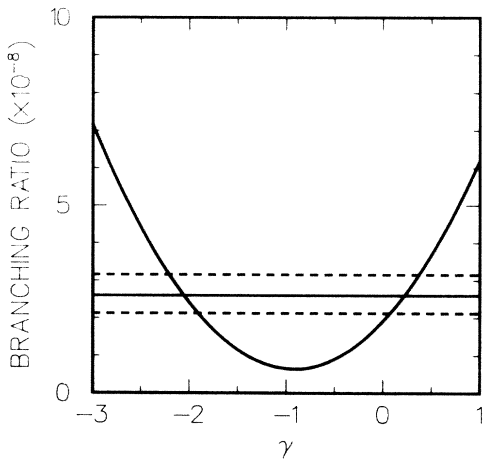

FIG. 3. The branching ratio for $\pi^+ \rightarrow e^+\nu_e\gamma$ as a function of γ for the cross-hatched region of the Dalitz plot in Fig. 1. The horizontal line indicates the measured branching ratio with the $\pm 1\sigma$ values shown as dotted lines.

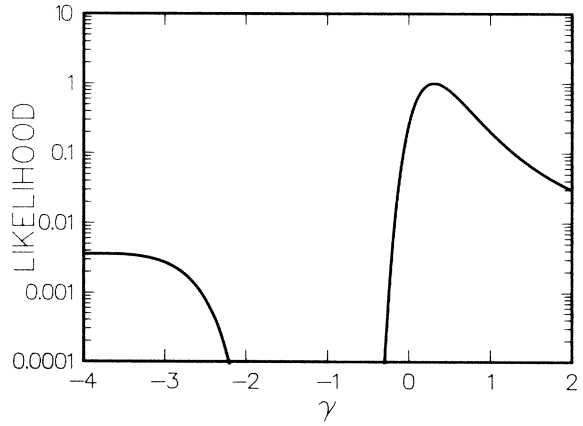

FIG. 4. The likelihood functions vs γ. The vertical scale is arbitrary.

$\gamma \simeq 0 \pm 0.3$. Earlier calculations yield a wide variety of results, as discussed in Ref. 11.

This experiment has resolved the quadratic ambiguity in the experimental determination of γ. Now that a unique, precise experimental value for γ is available, additional theoretical work is needed to use this result as a test of nonperturbative QCD calculations.

We wish to thank the many people at each of our institutions whose hard work made this experiment a success. This work was supported in part by the U. S. Department of Energy and the National Science Foundation.

Note added.—Our results agree with recent experiments at the Swiss Institute for Nuclear Research studying $\pi^+ \rightarrow e^+\nu\gamma$ [14] and $\pi^+ \rightarrow e^+\nu e^+ e^-$.[15]

---

[a]Present address: Physics Department, Princeton University, Princeton, NJ 08540.

[b]Present address: Elektrowatt Ing. AG, Zurich, Switzerland.

[c]Present address: Lockheed Missiles and Space Company, Palo Alto, CA 94304.

[1]D. A. Bryman, P. Depommier, and C. Leroy, Phys. Rep. **88**, 151 (1982).

[2]D. A. Bryman *et al.*, Phys. Rev. D **33**, 1211 (1986).

[3]V. G. Vaks and B. L. Ioffe, Nuovo Cimento **10**, 34 (1958); N. Cabibbo, Nuovo Cimento **11**, 837 (1959); S. A. Bludman and J. A. Young, Phys. Rev. **124**, 2037 (1960).

[4]H. W. Atherton *et al.*, Phys. Lett. **158B**, 81 (1985).

[5]R. P. Feynman and M. Gell-Mann, Phys. Rev. **109**, 193 (1958).

[6]P. Depommier, J. Heintze, C. Rubbia, and V. Soergel, Phys. Lett. **7**, 285 (1963).

[7]A. Stetz *et al.*, Nucl. Phys. **B4**, 189 (1978).

[8]J.-P. Perround, reported at the Tenth International Conference on Particles and Nuclei, Heidelberg, 1984 (unpublished).

[9]R. D. Bolton *et al.*, Phys. Rev. Lett. **53**, 1415 (1984).

[10]R. L. Ford and W. R. Nelson, Stanford Linear Accelerator Center Report No. SLAC 210, 1978 (unpublished).

[11]B. R. Holstein, Phys. Rev. D **33**, 3316 (1986).

[12]N. Paver and M. D. Svadron, Nuovo Cimento **78A**, 159 (1983).

[13]N. F. Nasrallah, N. A. Papadopoulos, and K. Schilcher, Phys. Lett. **113B**, 61 (1982).

[14]A. Bay *et al.*, Phys. Lett. **174B**, 455 (1986).

[15]S. Egli *et al.*, Phys. Lett. **175B**, 97 (1986).

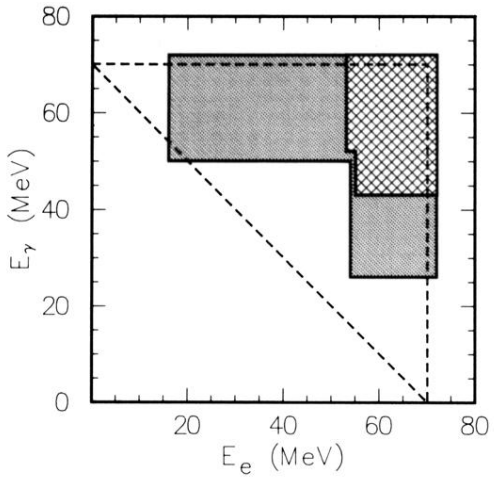

FIG. 1. The regions of the Dalitz plot used in this experiment. The cross-hatched region is used to determine γ from the observed number of $\pi^+ \rightarrow e^+ \nu_e \gamma$ events. The shaded and cross-hatched regions are used in the maximum-likelihood fit. The triangle indicates the limits of phase space assuming perfect measurement resolution.